Phase Equations for Quasi-Periodic Oscillators

Alper Demir[†]   Chenjie Gu[*]   Jaijeet Roychowdhury[*]

Koç University[†]   University of California[*]
Istanbul, Turkey   Berkeley, CA, USA

Abstract—**Oscillations and rhythmic activity are seen in natural and man-made systems. Dynamics of oscillators can be compactly described by phase domain models. Phase equations for periodic, single-frequency oscillators have been developed and utilized in analyzing oscillation phenomena that arise in electronic systems, circadian clocks, and the nervous system. We consider quasi-periodic oscillators and present a general phase model theory and numerical techniques for the construction of phase equations for multi-frequency oscillators. We demonstrate the utility of these phase equations in analyzing oscillators experiencing perturbations.**

I. INTRODUCTION

Autonomous rhythmic activity is observed everywhere in nature and man-made systems, e.g., in celestial mechanics, biology, electronics [1], [2]. Oscillation phenomena are best analyzed through the use of canonical phase domain models. Phase equations for periodic (single-frequency) oscillators have been developed and heavily utilized in analyzing weakly perturbed and coupled oscillators [1], [3]–[7]. It appears that a phase equation for periodic oscillators has first been derived by Malkin [3], [5] and re-discovered later by researchers in various disciplines. On the other hand, oscillations seen in nature and engineered systems are rarely perfectly periodic, but rather have a quasi-periodic nature. Even though the phase equation theory for periodic oscillators is well developed with abundant literature on the topic, phase models for quasi-periodic oscillators do not seem to have received much attention, with one notable exception: In [2], Izhikevich uses phase models for coupled quasi-periodic oscillators in order to investigate the mechanisms behind multiplexing in the brain. However, the phase model theory presented in [2] is not constructive, i.e., the form of the phase equations for a quasi-periodic oscillator is established but no theory and/or numerical techniques are offered for the construction of a phase model for a given oscillator. In [2], Izhikevich is interested in arriving at general results on the properties of coupled quasi-periodic oscillator networks based solely on the *form* of the phase model, without determining the functions that appear in the phase equations for a specific oscillator. Izhikevich [2] verifies the analytical results he obtains based on the form of the phase equations through time-domain, brute-force simulations of the coupled quasi-periodic oscillator network. Malkin's theory on the reduction of weakly perturbed oscillators to their phase models [3], as summarized by the Malkin theorem given in [5], is constructive and rather general but does not seem to capture the case of quasi-periodic oscillators.

In this paper, we present a general theory and numerical techniques for the construction of phase models for quasi-periodic oscillators. Unlike the phase model theory developed by Izhikevich in [2], our treatment is constructive, i.e., we not only establish the form of the phase equations but also describe exactly how one can compute and normalize the functions that appear in the phase model for a given oscillator. Our quasi-periodic phase model captures the previously known periodic model as a special case.

Quasi-periodic oscillators typically arise in the form of coupled single-frequency oscillators as a composite system. As such, one could construct a phase model for such an oscillator by simply composing the phase models for the periodic oscillator components. However, this requires the removal of the nonlinear coupling between the periodic oscillator components, which is usually the reason behind interesting dynamical behavior one may otherwise not observe in periodic oscillators. The generalization of the phase model theory from the periodic to the quasi-periodic case is non-trivial and requires intricate theoretical machinery and numerical methods beyond that is needed for periodic oscillators. Our treatment is general and applies to any autonomous system of differential equations that possesses a stable, quasi-periodic solution, i.e., the multi-frequency oscillator need not be constructed as a coupled system of single-frequency oscillators.

In Section II, we review the phase model theory for periodic oscillators. In Section III, we present our novel results on the constructive theory of phase equations for quasi-periodic oscillators. In Section IV, we describe the numerical techniques we employ in constructing a phase model for a quasi-periodic oscillator described by an autonomous system of differential equations. Finally, in Section V, we present results on two quasi-periodic oscillators, and demonstrate how one can use, i.e., numerically solve, the phase equations constructed in analyzing quasi-periodic oscillators experiencing perturbations.

II. REVIEW OF PHASE MODEL FOR PERIODIC OSCILLATORS

Let the system of ODEs

$$\frac{\mathrm{d}}{\mathrm{d}t}\mathbf{x} = \mathbf{f}(\mathbf{x}) \tag{1}$$

where $\mathbf{x} \in \mathbb{R}^N$ and $\mathbf{f} : \mathbb{R}^N \to \mathbb{R}^N$ describe an autonomous system. Let $\mathbf{x}_s(t)$ be a periodic solution of (1) that corresponds to an asymptotically orbitally stable limit cycle with the asymptotic phase property [8]. Then, define

$$\mathbf{G}(t) = \frac{\mathrm{d}\,\mathbf{f}(\mathbf{x})}{\mathrm{d}\mathbf{x}}\bigg|_{\mathbf{x}=\mathbf{x}_s(t)} \tag{2}$$

and $\mathbf{v}(t)$ as the periodic solution of the adjoint variational equation

$$\frac{\mathrm{d}}{\mathrm{d}t}\mathbf{z} = -\mathbf{G}^T(t)\,\mathbf{z} \tag{3}$$

satisfying the normalization condition

$$\mathbf{v}^T(t)\,\frac{\mathrm{d}\,\mathbf{x}_s(t)}{\mathrm{d}t} = 1 \tag{4}$$

$\mathbf{v}(t)$ is called the *Perturbation Projection Vector (PPV)* [9], entries of which are the infinitesimal *Phase Response Curves (PRCs)* [6].

Consider a perturbed version of the autonomous oscillator equations in (1)

$$\frac{\mathrm{d}}{\mathrm{d}t}\mathbf{x} = \mathbf{f}(\mathbf{x}) + \mathbf{b}(t) \tag{5}$$

with $\mathbf{b}(t) = 0$ for $t < 0$, where the perturbation $\mathbf{b}(t)$ is assumed to be "small" enough so that the solution of (1) does not wander off too far away from the limit cycle represented by $\mathbf{x}_s(t)$. Our goal is to approximately characterize the solution of the perturbed equations in (5) with a *phase equation*. The form and meaning of the phase equation is captured by the theorem below, stating that if

the perturbation in (5) is projected using the PPV $\mathbf{v}(t)$, then a phase-shifted version of $\mathbf{x}_s(t)$ characterizes the perturbed solution for the oscillator:

Theorem 2.1 ([7],[6]): Let $\alpha \in \mathbb{R}$, a scalar phase shift, satisfy the following nonlinear ODE

$$\frac{\mathrm{d}}{\mathrm{d}t}\,\alpha = \mathbf{v}^T(t+\alpha)\,\mathbf{b}(t) \tag{6}$$

with the initial condition $\alpha(t=0) = 0$. Then, the phase shifted solution $\mathbf{x}_s(t+\alpha(t))$ satisfies the perturbed oscillator equations

$$\frac{\mathrm{d}}{\mathrm{d}t}\mathbf{x} = \mathbf{f}(\mathbf{x}) + \left[\mathbf{v}^T(t+\alpha)\,\mathbf{b}(t)\right]\mathbf{u}(t+\alpha) \tag{7}$$

where $\mathbf{u}(t) = \frac{\mathrm{d}\,\mathbf{x}_s(t)}{\mathrm{d}t}$.

The scalar phase shift α and the nonlinear phase equation in (6) capture the deviations of the oscillator along the limit cycle. A perturbed oscillator also exhibits orbital deviations. However, phase deviations are deemed to be more important in applications, since they are persistent, i.e., they do not decay to zero after the perturbations are removed, whereas orbital deviations do. The scalar phase model for an oscillator serves as the ultimate *reduced-order* model.

III. PHASE MODEL FOR QUASI-PERIODIC OSCILLATORS

A. Preliminaries

Let $\mathbf{x}(t)$ be a quasi-periodic solution of the autonomous system in (1), expressed as follows

$$\mathbf{x}(t) = \check{\mathbf{x}}(\omega_1 t, \dots, \omega_p t) \tag{8}$$

where $\check{\mathbf{x}}(\theta_1, \dots, \theta_p) : \mathbb{T}^p \rightarrow \mathbb{R}^N$ is a *torus function*, that is, $\check{\mathbf{x}}$ is defined on the p-dimensional square $\mathbb{T}^p = [0, 2\pi]^p$ and it is 2π-periodic in each of its arguments θ_i, $i = 1, \dots, p$ [10]–[13]. ω_i for $i = 1, \dots, p$ are the basic frequencies (assumed to be incommensurate) of $\mathbf{x}(t)$ and the tuple $\boldsymbol{\omega} = [\omega_1, \dots, \omega_p]$ is called the frequency base. From now on, we will use the short hand notations $\check{\mathbf{x}}(\boldsymbol{\omega}\,t) = \check{\mathbf{x}}(\omega_1 t, \dots, \omega_p t)$, $\check{\mathbf{x}}(\boldsymbol{\theta}) = \check{\mathbf{x}}(\theta_1, \dots, \theta_p)$ and $\boldsymbol{\theta} = \boldsymbol{\omega}\,t$ wherever appropriate.

We assume that the quasi-periodic solution $\mathbf{x}(t)$ is stable in the following sense: When disturbed by a small amount, the solution of (1) asymptotically returns to the torus represented by $\check{\mathbf{x}}(\boldsymbol{\theta})$, making it a *normally hyperbolic invariant manifold* for the flow represented by (1) [14], [15]. In the case when $p = 1$, i.e., when the solution is periodic, this stability notion reduces to *asymptotic orbital stability* [8], and the invariant manifold becomes a limit cycle.

A torus function $\check{\mathbf{x}}(\boldsymbol{\theta})$ that satisfies the nonlinear PDE

$$\sum_{i=1}^{p} \omega_i \frac{\partial\,\check{\mathbf{x}}(\boldsymbol{\theta})}{\partial \theta_i} = \mathbf{f}(\check{\mathbf{x}}(\boldsymbol{\theta})) \tag{9}$$

in fact corresponds to a quasi-periodic solution $\mathbf{x}(t) = \check{\mathbf{x}}(\boldsymbol{\omega}\,t)$ of (1) [11]–[13]. The PDE above can be solved as a periodic boundary value (BVP) problem using a spectral method based on Fourier series representations for the dependence of $\check{\mathbf{x}}(\boldsymbol{\theta})$ on each of θ_i (e.g., the multi-tone harmonic balance (HB) method) [11], [13], or the multi-time finite-difference time-domain (MTFDTD) technique [11], [12], with appropriate *phase conditions* [12], [13]. Here, we note

$$\frac{\mathrm{d}\,\mathbf{x}(t)}{\mathrm{d}t} = \frac{\mathrm{d}\,\check{\mathbf{x}}(\boldsymbol{\omega}\,t)}{\mathrm{d}t} = \sum_{i=1}^{p} \omega_i \frac{\partial\,\check{\mathbf{x}}(\boldsymbol{\theta})}{\partial \theta_i}\bigg|_{\boldsymbol{\theta}=\boldsymbol{\omega}\,t} = \mathbf{f}(\check{\mathbf{x}}(\boldsymbol{\omega}\,t)) \tag{10}$$

which follows from the total derivative of $\check{\mathbf{x}}(\boldsymbol{\omega}\,t)$ with respect to t.

B. Variational (Linearized) System

The variational (linearized) system associated with (1) and the solution $\mathbf{x}(t)$ is given by

$$\frac{\mathrm{d}}{\mathrm{d}t}\mathbf{y} = \mathbf{G}(t)\,\mathbf{y} \tag{11}$$

where $\mathbf{G}(t)$ is defined as in (2), but evaluated at $\mathbf{x}(t)$ instead. Since $\mathbf{G}(t)$ is now quasi-periodic, we define the torus matrix function

$$\check{\mathbf{G}}(\boldsymbol{\theta}) = \frac{\mathrm{d}\,\mathbf{f}(\mathbf{x})}{\mathrm{d}\mathbf{x}}\bigg|_{\mathbf{x}=\check{\mathbf{x}}(\boldsymbol{\theta})} \tag{12}$$

and hence $\mathbf{G}(t) = \check{\mathbf{G}}(\boldsymbol{\omega}\,t)$. The following result serves as the *key* in deriving a phase model for a quasi-periodic oscillator:

Theorem 3.1 (Coppel [15] (page 84), Samoilenko [10] (page 72)): Each and every one of the p partial derivatives (all quasi-periodic)

$$\frac{\partial\,\check{\mathbf{x}}(\boldsymbol{\theta})}{\partial \theta_i}\bigg|_{\boldsymbol{\theta}=\boldsymbol{\omega}\,t} \triangleq \mathbf{u}_i(t) \triangleq \check{\mathbf{u}}_i(\boldsymbol{\omega}\,t) \tag{13}$$

is a solution of the homogeneous variational system in (11), where $\check{\mathbf{u}}_i$ is the torus function that corresponds to $\mathbf{u}_i$.

We omit the proof of this nontrivial result due to space constraints but note that it can not be obtained by simply computing the time derivatives of both sides of (1), resulting in (see also (10))

$$\frac{\mathrm{d}}{\mathrm{d}t}\left[\sum_{i=1}^{p} \omega_i \frac{\partial\,\check{\mathbf{x}}(\boldsymbol{\theta})}{\partial \theta_i}\bigg|_{\boldsymbol{\theta}=\boldsymbol{\omega}\,t}\right] = \check{\mathbf{G}}(\boldsymbol{\omega}\,t) \sum_{i=1}^{p} \omega_i \frac{\partial\,\check{\mathbf{x}}(\boldsymbol{\theta})}{\partial \theta_i}\bigg|_{\boldsymbol{\theta}=\boldsymbol{\omega}\,t} \tag{14}$$

Based on the above, we can conclude that $\sum_{i=1}^{p} \omega_i \frac{\partial\,\check{\mathbf{x}}(\boldsymbol{\theta})}{\partial \theta_i}\big|_{\boldsymbol{\theta}=\boldsymbol{\omega}\,t}$ is a solution of (11), but can not arrive at Theorem 3.1. On the other hand, (14) is a simple corollary of Theorem 3.1, because any linear combination of the solutions of (11) is also a solution.

We assume that the p quasi-periodic solutions of (11) characterized by Theorem 3.1 are linearly independent [10], [15], which can be obtained easily by (numerically) computing the partial derivatives once the torus function $\check{\mathbf{x}}(\boldsymbol{\theta})$ is computed. The quasi-periodic solutions of (11) will all lie in the null space of the Jacobian of the (un-augmented) set of nonlinear algebraic equations one solves in the multi-tone HB or the MTFDTD method. With p linearly independent solutions, these Jacobians have a p-dimensional null space, making it necessary to augment the multi-tone HB and the MTFDTD equations with p phase conditions in order to remove the freedom in the *phases* of $\check{\mathbf{x}}(\boldsymbol{\theta})$ and obtain a unique solution for (9) [12], [13].

A torus function $\check{\mathbf{u}}(\boldsymbol{\theta})$ representing a quasi-periodic solution $\mathbf{u}(t)$ of (11) satisfies the linear PDE (with periodic boundary conditions)

$$\sum_{i=1}^{p} \omega_i \frac{\partial\,\check{\mathbf{u}}(\boldsymbol{\theta})}{\partial \theta_i} = \check{\mathbf{G}}(\boldsymbol{\theta})\,\check{\mathbf{u}}(\boldsymbol{\theta}) \tag{15}$$

similar to (9). Hence, the torus functions $\check{\mathbf{u}}_i(\boldsymbol{\theta})$ for $i = 1, \dots, p$ representing p quasi-periodic solutions of (11) lie in, and span, the null space of the linear operator (with periodic boundary conditions)

$$\left[\sum_{i=1}^{p} \omega_i \frac{\partial\,\cdot}{\partial \theta_i}\right] - \check{\mathbf{G}}(\boldsymbol{\theta}) \tag{16}$$

which corresponds to the un-augmented Jacobian of the multi-tone HB or the MTFDTD method.

C. Adjoint Variational (Linearized) System

We next consider the *adjoint* variational equation in (3). Based on the null space argument above, (3) will also have p linearly independent quasi-periodic solutions. Unfortunately, there is no simple procedure through which one can obtain these solutions for the adjoint equation. One has to either solve an eigenvalue problem (Section IV-B) or use another appropriate technique to compute a

p-dimensional basis set for the adjoint null space of the multi-tone HB or the MTFDTD Jacobian. We denote the linearly independent quasi-periodic solutions of the adjoint equation with

$$\mathbf{v}_i(t) \triangleq \breve{\mathbf{v}}_i(\boldsymbol{\omega}\, t) \tag{17}$$

for $i = 1, \ldots, p$. The torus functions $\breve{\mathbf{v}}_i(\boldsymbol{\theta})$ satisfy the adjoint of the PDE in (15) and span the null space of the linear operator

$$\left[\sum_{i=1}^{p} \omega_i \frac{\partial \cdot}{\partial \theta_i} \right] + \breve{\mathbf{G}}^T(\boldsymbol{\theta}) \tag{18}$$

D. Solutions of Variational (Linearized) Systems

We note that not all of the solutions of the forward variational equation in (11) and the adjoint equation in (3) are quasi-periodic. The quasi-periodic solutions span a p-dimensional subspace, however, the total solution space has dimension $N > p$. We assume that the solutions of (11) that lie in the complementary $N - p$-dimensional subspace are all decaying solutions which do not persist. This, among other things, guarantees that the quasi-periodic solution $\mathbf{x}(t)$ of (1) is stable in the sense discussed before. Based on Floquet theory for quasi-periodic linear systems [15], [16], under some conditions, the solutions of (11) and (3) can be represented in the following forms

$$\mathbf{y}(t) = \mathbf{u}(t)\, e^{\mu\, t} \qquad \mathbf{z}(t) = \mathbf{v}(t)\, e^{-\mu\, t} \tag{19}$$

where $\mathbf{u}(t)$ and $\mathbf{v}(t)$ are quasi-periodic and μ is the Floquet exponent. For a quasi-periodic solution, $\mu = 0$, and for all of the other modes, $\mathrm{Re}\,\{\mu\} < 0$. The (linearly independent) solutions of the variational equations can be obtained by computing all of the eigenvalues and eigenfunctions of the operators in (16) and (18).

E. Perturbation Projection Vectors (PPVs) and Normalization

The p linearly independent quasi-periodic solutions of the adjoint equation serve as the *perturbation projection vectors* (PPVs) for the p phases of the quasi-periodic oscillator. In order for the perturbation projection operations to be correct, the following bi-orthogonality relationships (i.e., normalization conditions)

$$\mathbf{v}_i^T(t)\, \mathbf{u}_j(t) = \delta_{ij} \tag{20}$$

among solutions of the forward and adjoint equation need to be satisfied at all t and for $i, j = 1, \ldots, p$. When the solutions of the adjoint equation are computed as a basis set for the null space of the operator in (18), they do not necessarily satisfy the above normalization conditions. These normalization conditions need to be explicitly enforced. We note here that any solution $\mathbf{y}(t)$ of the forward variational equation in (11) and a solution $\mathbf{z}(t)$ of the adjoint equation in (3) satisfy

$$\frac{\mathrm{d}}{\mathrm{d}t} \left[\mathbf{z}^T(t)\, \mathbf{y}(t) \right] = 0 \tag{21}$$

As such, if we enforce the bi-orthogonality conditions in (20) at some chosen t^*, then they are guaranteed to hold at all other t due to (21). We enforce the bi-orthogonality conditions not directly on the quasi-periodic solutions $\mathbf{u}_j(t)$ and $\mathbf{v}_i(t)$ but rather on the corresponding torus functions $\breve{\mathbf{u}}_j(\boldsymbol{\theta})$ and $\breve{\mathbf{v}}_i(\boldsymbol{\theta})$. We use the multi-argument torus functions to compactly represent the quasi-periodic solutions, as there is no compact representation for a quasi-periodic solution as a function of time. In order to attain a simple condition that will be directly enforced on the torus functions, we make use of the following fact: The domain of the torus functions, i.e., the p-dimensional square $\mathbb{T}^p$, is *densely covered* by $\boldsymbol{\theta} = \boldsymbol{\omega}\, t$: For every $\boldsymbol{\theta}^*$ in the p-dimensional square $\mathbb{T}^p$, there exists a t^* such that $\boldsymbol{\theta}^* = \boldsymbol{\omega}\, t^* \mod 2\pi$, since the basic frequencies in $\boldsymbol{\omega}$ are incommensurate. Similarly, the torus that is represented by $\breve{\mathbf{x}}(\boldsymbol{\theta})$ is densely covered by the quasi-periodic solution $\mathbf{x}(t)$ [13]. Thus, we

can choose to enforce the bi-orthogonality conditions at any $\boldsymbol{\theta}^*$ in the p-dimensional square $\mathbb{T}^p$. Then they will also hold at all other points in $\mathbb{T}^p = [0, 2\pi]^p$, due to (21). However, instead of enforcing the normalization conditions at a chosen $\boldsymbol{\theta}^*$, we enforce them on an average taken over all $\boldsymbol{\theta} \in \mathbb{T}^p$. Even though the two are equivalent in exact arithmetic, the latter will have better numerical properties. In order to enforce (20) as such, we first compute the torus functions $\breve{\mathbf{v}}_i(\boldsymbol{\theta})$ for $i = 1, \ldots, p$, by computing a basis set for the null space of the operator in (18). We then compute the average (over $\mathbb{T}^p$) of the $p \times p$ matrix formed by the inner products of $\breve{\mathbf{v}}_i(\boldsymbol{\theta})$ for $i = 1, \ldots, p$ and $\breve{\mathbf{u}}_j(\boldsymbol{\theta}) = \frac{\partial\, \breve{\mathbf{x}}(\boldsymbol{\theta})}{\partial \theta_j}$ for $j = 1, \ldots, p$. Making use of the QR decomposition of this inner product matrix, we compute a new set of $\breve{\mathbf{v}}_i(\boldsymbol{\theta})$ as a linear combination of $\breve{\mathbf{v}}_i(\boldsymbol{\theta})$. The new $\breve{\mathbf{v}}_i(\boldsymbol{\theta})$ not only satisfy (20) but also represent p linearly independent quasi-periodic solutions for the adjoint equation.

We note here that the orthogonality of $\breve{\mathbf{v}}_i(\boldsymbol{\omega}\, t)$ for $i = 1, \ldots, p$ to all of the decaying modes of the forward variational equation is also required but need not be enforced explicitly. The decaying modes of the variational equation are the eigenfunctions of the operator in (16) that correspond to nonzero eigenvalues. $\breve{\mathbf{v}}_i(\boldsymbol{\omega}\, t)$ for $i = 1, \ldots, p$ are the eigenfunctions of the adjoint of this operator in (18) that correspond to zero eigenvalues. An operator and its adjoint have the same eigenvalues, and their eigenfunctions that correspond to *different* eigenvalues are always orthogonal to each other. Thus, $\breve{\mathbf{v}}_i(\boldsymbol{\omega}\, t)$ are guaranteed to be orthogonal to all of the decaying modes of the forward variational equation. However, the above property does not hold for the eigenfunctions that correspond to the same eigenvalue. In particular, if an eigenvalue is repeated, the corresponding eigenfunctions of the operator and its adjoint are not guaranteed to be bi-orthogonal, hence all the trouble we had to go through above.

F. Phase Equations for Quasi-Periodic Oscillators

We now consider a perturbed quasi-periodic oscillator. Our goal is again to approximately characterize the solution of (5), as in Section II, but with a generalized *phase model* that is valid for quasi-periodic oscillators. We next reveal the form of the phase equations for a quasi-periodic oscillator and show that a (multi) phase shifted version of the quasi-periodic solution $\mathbf{x}(t)$ satisfies the oscillator equations in (5) with the perturbation projected onto the persistent quasi-periodic modes of the variational equation. The theorem below captures the main result of this paper and is the generalization of Theorem 2.1 to the quasi-periodic case:

Theorem 3.2: Let $\alpha_i \in \mathbb{R}$ for $i = 1, \ldots, p$ be the p phase shifts and satisfy the following set of coupled nonlinear ODEs

$$\frac{\mathrm{d}}{\mathrm{d}t}\, \alpha_i = \frac{1}{\omega_i} \breve{\mathbf{v}}_i^T(\omega_1(t + \alpha_1), \ldots, \omega_p(t + \alpha_p))\, \mathbf{b}(t) \tag{22}$$

with initial conditions $\alpha_i(t = 0) = 0$, written compactly as

$$\frac{\mathrm{d}}{\mathrm{d}t}\, \alpha_i = \frac{1}{\omega_i} \breve{\mathbf{v}}_i^T(\boldsymbol{\omega}.(t + \boldsymbol{\alpha}))\, \mathbf{b}(t) \tag{23}$$

where $\boldsymbol{\alpha} = [\alpha_1, \ldots, \alpha_p]$ and $t + \boldsymbol{\alpha} = [t + \alpha_1, \ldots, t + \alpha_p]$. Then, the (multi) phase shifted quantity $\breve{\mathbf{x}}(\boldsymbol{\omega}.(t + \boldsymbol{\alpha}))$ satisfies the perturbed oscillator equations

$$\frac{\mathrm{d}}{\mathrm{d}t}\mathbf{x} = \mathbf{f}(\mathbf{x}) + \sum_{i=1}^{p} \left[\breve{\mathbf{v}}_i^T(\boldsymbol{\omega}.(t + \boldsymbol{\alpha}))\, \mathbf{b}(t) \right] \breve{\mathbf{u}}_i(\boldsymbol{\omega}.(t + \boldsymbol{\alpha})) \tag{24}$$

Above, $\breve{\mathbf{x}}(\boldsymbol{\omega}\, (t))$ without the phase shifts represents the quasi-periodic solution of the unperturbed oscillator equations in (1).

We omit the proof of the above theorem due to space constraints.

IV. NUMERICAL METHODS

A. Computing Quasi-Periodic Solution of the Oscillator

In order to construct the phase model for a quasi-periodic oscillator, we need to first compute its large-signal quasi-periodic solution. We use the MTFDTD [11], [12] method in solving the system of PDEs in (9) along with periodic boundary conditions in p phases in order to obtain a discretized version of the torus function in (8), where the partial derivatives in (9) are approximated with finite-difference formulas. In particular, we use the 2nd to 6th order central finite-difference schemes given in Schilder *et.al.* [12]. For simplicity, we discretize the torus function in (8) using a uniform grid in each phase variable, with M_i equidistant points for θ_i between 0 and $2\pi \frac{M_i - 1}{M_i}$, noting that the torus function is 2π-periodic in θ_i for $i = 1, \ldots, p$. Thus, we end up with $N \prod_{i=1}^{p} M_i$ unknowns at the mesh points. With the finite-difference discretization of the PDE in (9) evaluated at each one of the mesh points, we obtain $N \prod_{i=1}^{p} M_i$ nonlinear algebraic equations. However, the p frequencies ω_i in (9) also need to be included among the unknowns. Usually, p phase conditions are employed to augment the equations obtained in order to obtain a square system of nonlinear algebraic equations [12]. These phase conditions remove the freedom in the p phases of the autonomous quasi-periodic system and result in a unique solution. The square system of nonlinear algebraic equations are then usually solved with Newton's method.

1) Phase conditions versus least-squares solution: In our implementation, we follow Schilder *et.al.* [13] and do not employ phase conditions. Instead, we form a rectangular system of equations with $p + N \prod_{i=1}^{p} M_i$ unknowns, including the p unknown frequencies, and the $N \prod_{i=1}^{p} M_i$ equations obtained from finite-difference discretization. We use the Newton's method in order to solve this rectangular system of nonlinear algebraic equations. At every iteration of Newton's method, we solve the under-determined, rectangular system of linear(ized) equations using a least-squares approach that is equivalent to using the Moore-Penrose pseudo-inverse of the rectangular Jacobian matrix. In order to exploit the sparsity of the Jacobian matrix, we use an iterative least-squares linear system solution technique, namely LSQR [17] as implemented in Matlab. LSQR is a conjugate-gradient type method for solving sparse linear equations and sparse least-squares problems of the form $\mathbf{A}\,\mathbf{x} = \mathbf{b}$, based on minimizing $||\mathbf{A}\,\mathbf{x} - \mathbf{b}||^2 + d^2 ||\mathbf{x}||^2$ where d is a damping parameter [17]. We note here that the under-determined, rectangular linear system of equations that we solve at every Newton iteration has a solution but not unique. When we solve this equation in the least-squares sense with LSQR, we are computing the solution that has the smallest Euclidean norm. In this under-determined case, the "least-squares" refers to the norm of the solution instead of the norm of the residual that would have made sense for an over-determined system. The minimum norm solution makes sense in the context of Newton's method, since the Newton *increment* should converge to the zero vector as the Newton iterates converge to the solution of the nonlinear equations. The least-squares solution of the linearized equations at every Newton iteration and the initial guess provided for Newton's method, in effect, correspond to enforcing phase conditions and yield one of the infinitely many quasi-periodic solutions for the autonomous oscillator.

2) Robust convergence for Newton's method and generating an initial guess: In order to obtain robust convergence in Newton's method, we try to supply a good initial guess for the solution and/or use a continuation scheme. We generate an initial guess for the torus function by first performing a "long" transient, time-domain numerical simulation. We then perform NAFF (Numerical Analysis of Fundamental Frequencies) [18] analysis (as implemented in the SDDS toolkit from Argonne National Laboratory [19]) on the time series data from time-domain simulation in order to extract a quasi-

periodic approximation to be used in constructing an initial guess for the torus function. NAFF [18], which was developed in order to analyze time series data in galactic dynamics, extracts the frequencies and the corresponding complex amplitudes iteratively, one at a time, by deflating the frequency components already extracted and performing orthogonal projections. NAFF [18] had been proved to be more accurate than using simple FFTs: The accuracy of the frequencies obtained by NAFF improves with the fourth power of the length of the time series data. NAFF provides only a set of frequencies with corresponding complex amplitudes for the waveforms produced by transient analysis. This data is then post-processed in order to extract the fundamental frequencies and form a discretized form of the torus function in (8) to be used as an initial guess for Newton's method. When the initial guess generated as such is not good enough in achieving robust convergence we employ a problem, i.e., oscillator, specific continuation scheme. Globally convergent, robust and automatic techniques for computing quasi-periodic solutions of autonomous dynamical systems is an open problem and beyond the scope of this paper.

B. Computing the Quasi-Periodic Perturbation Projection Vectors

In order to compute and correctly normalize the PPVs that are needed in constructing the phase model, we follow the procedure that was outlined in Section III-E. The partial derivatives of the torus function are computed using the same finite-difference formula that was employed in discretizing the PDEs in (9). In order to compute the un-normalized PPVs, we compute p basis vectors for the null space of the transpose of the MTFDTD Jacobian. The MTFDTD Jacobian we use here is a square matrix with dimension $N \prod_{i=1}^{p} M_i$, obtained by removing the extra p columns (that correspond to the unknown frequencies) from the rectangular Jacobian matrix that was used during Newton iterations.

For a set of basis vectors for the null space of the transpose of the sparse Jacobian matrix, we perform a partial eigen-decomposition using the *eigs* routine in Matlab in order to compute the p smallest magnitude eigenvalues (which are theoretically equal to zero) and the corresponding eigenvectors. *eigs* in Matlab is based on ARPACK (for Arnoldi Package) [20] which uses implicitly-restarted Arnoldi iterations in computing several eigenvalues and eigenvectors in large-scale eigenvalue problems. Arnoldi iterations tend to converge most rapidly to the extremal eigenvalues with the largest magnitude. In order to instead obtain the eigenvalues with the smallest magnitude, Arnoldi iterations are performed on the inverse of the matrix (without computing the inverse, using sparse Gaussian elimination for matrix-vector products). If the smallest eigenvalues are indeed equal to zero, this would of course run into numerical problems. However, the smallest eigenvalues are not exactly zero as a result of various numerical inaccuracies mostly due to finite-difference discretization of the operator in (18) and in computing the large-signal steady-state solution. As a result, Arnoldi iterations on the inverse of the Jacobian matrix proceeds without numerical problems. In cases where the smallest eigenvalues are small enough to cause numerical problems, one can use either a shift-and-invert scheme or a generalization of the matrix augmentation technique described in [9] to compute a set of basis vectors for the null space. After the raw PPVs are computed as described above, we follow the procedure described in Section III-E in order to normalize them.

C. Computing the Solution of the Phase Equations

With the numerically computed and properly normalized torus functions for the PPVs in hand, we have all we need in order to solve the phase equations in (22), which are a set of p coupled nonlinear ODEs for the p phase variables α_i for $i = 1, \ldots, p$. Given a perturbation $\mathbf{b}(t)$ waveform, we compute the solution of these
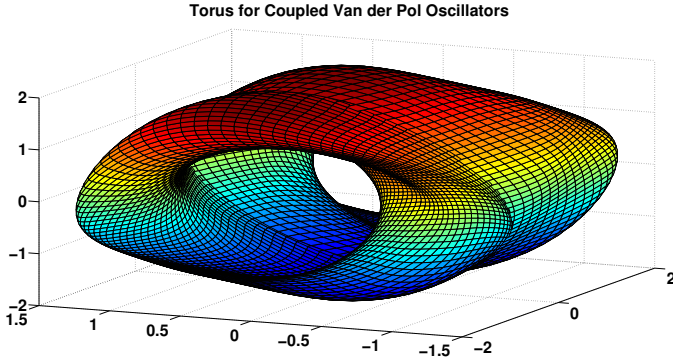
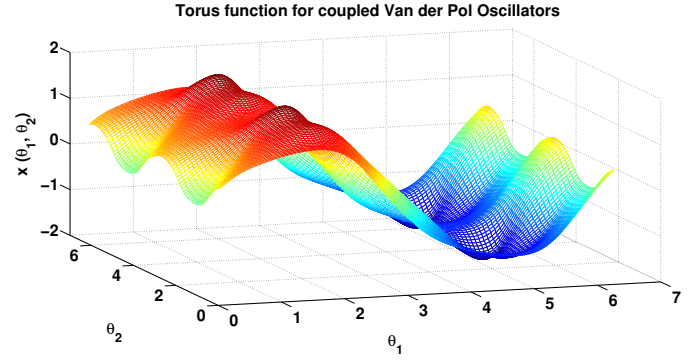Fig. 1. Torus for coupled Van der Pol oscillators

Fig. 2. Torus function for coupled Van der Pol oscillators

coupled ODEs using explicit Runge-Kutta formulas as implemented in *ode23* and *ode45* routines of Matlab. In the case when stiffness in solving these equations becomes an issue, one can use an implicit technique. We note here that the PPVs are not available analytically, they have been computed on a finite-difference mesh on the p-dimensional square $\mathbb{T}^p$. When we solve the phase equations, we use p-dimensional cubic interpolation to evaluate the torus functions for the PPVs at points not exactly on the finite-difference mesh points.

V. RESULTS

A. Coupled Van der Pol Oscillators

The following represents two coupled Van der Pol oscillators [13]

$$
\begin{aligned}
\ddot{x} - \epsilon\left(1 - x^2\right)\dot{x} + \gamma_1^2 x &= -\delta\left(ay^2 + bx^2y^2\right)\dot{x} \\
\ddot{y} - \epsilon\left(1 - y^2\right)\dot{y} + \gamma_2^2 y &= -\delta\left(\alpha x^2\right)\dot{y}
\end{aligned}
\tag{25}
$$

where δ and ϵ control the strength of nonlinear coupling and the degree of nonlinearity in the two oscillators. For $\delta = \epsilon = 0$, they become decoupled and degenerate into two linear harmonic oscillators. We set $\delta = \epsilon = 1$ and $\gamma_1 = 1$, $\gamma_2 = \sqrt{2}$, $a = 0.2$, $\alpha = 0.4$, and rewrite (25) above as a system of four, first-order differential equations. In order to compute the torus function $\breve{x}(\theta_1, \theta_2)$ that corresponds to the quasi-periodic solution of this oscillator system, we discretize the 2-dimensional square $\mathbb{T}^2$ with a uniform grid of $M \times M = 100 \times 100$ points resulting in a total of $40,000$ grid unknowns. The two fundamental frequencies ω_1 and ω_2 are also unknown. In approximating the partial derivatives in (9), we use a 6th order central finite difference scheme [12] with periodic boundary conditions. For Newton's method, we supply an initial guess based on the analytical solution of the oscillator system when $\delta = \epsilon = 0$. With this initial guess, we obtain robust, quadratic convergence in Newton's method without the need for a continuation scheme, with the residual norm reaching 10^{-13} in 8 iterations. The fundamental frequencies computed are $\omega_1 \approx 0.97155$ and $\omega_2 \approx 1.37287$. The function $\breve{x}(\theta_1, \theta_2)$ computed represents a torus in 4-D for this oscillator system. In Figure 1, this torus is shown in 3-D for three (out of four) state variables of this oscillator. In Figure 2, the torus function $\breve{x}(\theta_1, \theta_2)$ computed for one of the state variables can be seen. Next, we compute the torus functions for the PPVs $\breve{v}_i(\theta_1, \theta_2)$ for $i = 1, 2$ using the partial eigen-decomposition and normalization scheme described in Section IV-B. Then, we perform a perturbation analysis for the coupled Van der Pol oscillators with a perturbation

$$
b(t) = 10^{-3}[1 + \cos\left(\omega_2 t\right) + \sin\left(\omega_1 t\right)]
\tag{26}
$$

injected as an additive term to one of the differential equations. The phase shifts $\alpha_1(t)$ and $\alpha_2(t)$ for this perturbation that were computed by solving the phase equations in (22) as described in Section IV-C are shown in Figure 3. As it can be observed in this figure, the perturbation described above is on for $0 \leq t \leq 2000$
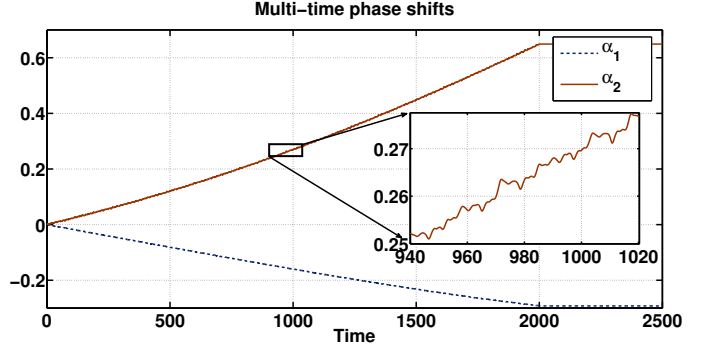

Fig. 3. Multi-time phase shifts for coupled Van der Pol oscillators

and turns of at $t = 2000$ and thereon the phase shifts remain constant. The waveforms for the phase shifts $\alpha_1(t)$, $\alpha_2(t)$ and the torus function $\breve{x}(\theta_1, \theta_2)$ for the steady-state solution can be used to construct the perturbed oscillator waveforms simply as $\breve{x}(\omega_1(t + \alpha_1(t)), \omega_2(t + \alpha_2(t)))$. In Figure 4, the waveform constructed as such for one of the state variables is shown along with the waveform $\breve{x}(\omega_1 t, \omega_2 t)$ constructed for an unperturbed oscillator. In this figure, there are two more waveforms obtained with full transient, time-domain simulation of the oscillator equations, one for the perturbed and the other for the unperturbed case. For these simulations, we choose the initial condition $\breve{x}(0, 0)$ so that these waveforms can be compared with the ones constructed directly from the torus function $\breve{x}(\theta_1, \theta_2)$. In Figure 4, the waveforms obtained with full time-domain simulation are in fact indistinguishable from the ones directly constructed. In Figure 5, the difference between the simulated and constructed waveforms are shown in a semi-log scale as the curves below the 10^{-2}-level. The curves above the 10^{-2}-level represent the difference between the waveforms of the perturbed and
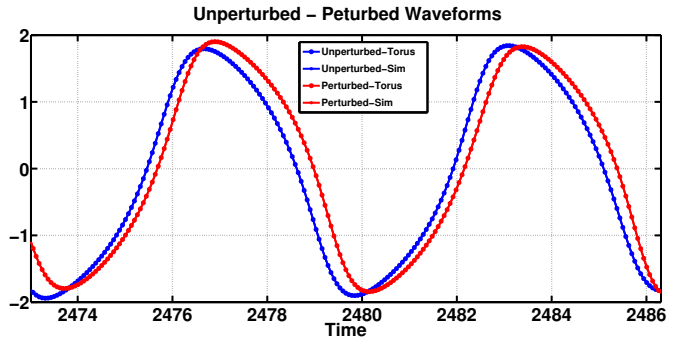

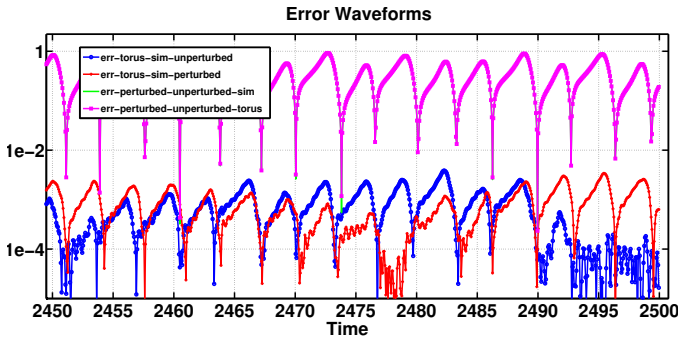Fig. 4. Perturbed waveforms for coupled Van der Pol oscillators

Fig. 5. Error waveforms for coupled Van der Pol oscillators

Fig. 6. Perturbed waveforms for Wilson-Cowan oscillators

unperturbed oscillator and are given for reference. As seen, the total phase shifts due to the perturbation are significant enough to result in a large difference between the waveforms of the perturbed and unperturbed oscillator. However, the waveforms constructed for the perturbed oscillator based on the solutions of the phase equations match very well with the waveforms obtained with full numerical simulations. This result serves as a verification for the correctness of our theory and numerical methods for phase equations of quasi-periodic oscillators.

B. Wilson-Cowan Oscillators

The following represents two (for $i = 1, 2$) coupled neural oscillators of the Wilson-Cowan type [2] that are used in brain modeling

$$\dot{x}_i = -x_i + S(\rho_i + ax_i - by_i + E_i)$$
$$\dot{y}_i = -y_i + S(\rho_y + cx_i - dy_i) \tag{27}$$

with

$$S(\rho) = \frac{1}{1 + e^{-\rho}} \tag{28}$$

$$E_1 = x_2 \qquad E_2 = x_1 \tag{29}$$

where the E_i term represents the coupling. For $a = b = c = 10$, $d = -2$, $\rho_y = -6$, $\rho_1 = -2$ and $\rho_2 = 2$, the above oscillator system exhibits multi-frequency oscillations [2].

We compute the torus function $\check{x}(\theta_1, \theta_2)$ that corresponds to the quasi-periodic solution of this oscillator system, again on a mesh with 100×100 grid points and using a 6th order scheme. For Newton's method, we generate an initial guess with a transient simulation followed with NAFF analysis as described in Section IV-A, and obtain robust, quadratic convergence with the residual norm reaching 10^{-13} in 6 iterations. The fundamental frequencies computed are $\omega_1 \approx 1.03650$ and $\omega_2 \approx 1.36820$. In Figure 6, we present perturbation analysis results similar to the ones presented in Figure 4 for a perturbation in the same form as in (26) but that turns off at $t = 500$ and with frequencies different from the fundamental frequencies of the oscillator system. As we observe in Figure 6, the multi-phase shifted waveform for a quasi-periodic oscillator can not be obtained by simply time-shifting the unperturbed waveforms. For single-frequency oscillators, phase shift translates directly into a time shift, but not for multi-frequency oscillators. The waveforms constructed for the perturbed oscillator based on the solutions of the phase equations again match very well with the waveforms obtained from full numerical simulations.

VI. CONCLUSION

We have presented a general phase model theory and numerical techniques for the construction of phase equations for quasi-periodic oscillators. We have demonstrated the utility of these phase equations
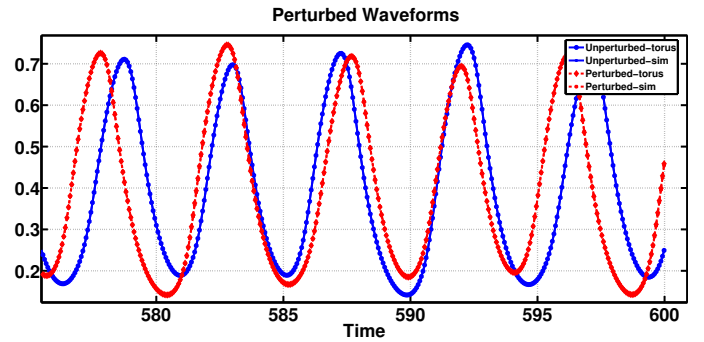
in analyzing quasi-periodic oscillators experiencing perturbations. The waveforms constructed for a perturbed multi-frequency oscillator based on the solutions of only several coupled phase equations can form an accurate depiction of the waveforms that would otherwise be obtained with full numerical simulations. The phase equations can serve as the ultimate reduced-order, compact model for multi-frequency oscillators.

REFERENCES

[1] Arthur T. Winfree. *The Geometry of Biological Time*. Springer, 2001.
[2] Eugene M. Izhikevich. Weakly connected quasi-periodic oscillators, FM interactions, and multiplexing in the brain. *SIAM Journal on Applied Mathematics*, 59(6):2193–2223, 1999.
[3] I.G. Malkin. Methods of Poincare and Liapunov in theory of non-linear oscillations. *Gostexizdat*, Moscow, 1949.
[4] Y. Kuramato. *Chemical Oscillations, Waves, and Turbulence*. Springer-Verlag, New York, 1984.
[5] F. C. Hoppensteadt and Eugene M. Izhikevich. *Weakly Connected Neural Networks*. Springer, 1997.
[6] E.M. Izhikevich. *Dynamical Systems in Neuroscience: The Geometry of Excitability and Bursting*. Chapter 10. MIT Press, 2007.
[7] A. Demir, A. Mehrotra, and J. Roychowdhury. Phase noise in oscillators: A unifying theory and numerical methods for characterisation. *IEEE Transactions on Circuits and Systems-I: Fundamental Theory and Applications*, 47(5):655–674, May 2000.
[8] M. Farkas. *Periodic Motions*. Springer-Verlag, 1994.
[9] A. Demir and J. Roychowdhury. A reliable and efficient procedure for oscillator PPV computation, with phase noise macromodelling applications. *IEEE Tran. on CAD of ICs and Systems*, 22(2):188–197, Feb 2003.
[10] A.M. Samoilenko. *Elements of the Mathematical Theory of Multi-Frequency Oscillations*. Kluwer Academic Publishers, 1991.
[11] J. Roychowdhury. Analyzing circuits with widely separated time scales using numerical PDE methods. *IEEE Transactions on Circuits and Systems: Fundamental Theory and Applications,*, 48(5):578 –594, May 2001.
[12] Frank Schilder, Hinke M. Osinga, and Werner Vogt. Continuation of quasi-periodic invariant tori. *SIAM Journal on Applied Dynamical Systems*, 4:459–488, 2005.
[13] Frank Schilder, Werner Vogt, Stephan Schreiber, and Hinke M. Osinga. Fourier methods for quasi-periodic oscillations. *International Journal for Numerical Methods in Engineering*, 67(5):629–671, 2006.
[14] Stephen Wiggins. *Normally Hyperbolic Invariant Manifolds in Dynamical Systems*. Springer, 1994.
[15] W.A. Coppel. *Dichotomies in Stability Theory*. Springer, 1978.
[16] L. Zhen-sheng. The Floquet theory for quasi-periodic linear systems. *Applied Mathematics and Mechanics*, 3(3):365–381, June 1982.
[17] C. C. Paige and M. A. Saunders. LSQR: An algorithm for sparse linear equations and sparse least squares. *TOMS*, 8(1):43–71, 1982.
[18] Jacques Laskar. Introduction to frequency map analysis. In Carlos Simo, editor, *Hamiltonian systems with three or more degrees of freedom*, pages 134–150. Kluwer Academic Publishers, 1999.
[19] M. Borl, L. Emery, H. Shang, and R. Soliday. Users Guide for SDDS Toolkit version 1.30, 2005.
[20] R.B. Lehoucq, D.C. Sorensen, and C. Yang. *ARPACK Users' Guide: Solution of Large-Scale Eigenvalue Problems with Implicitly Restarted Arnoldi Methods*. SIAM Publications, 1998.